Colloids and Surfaces B: Biointerfaces 181 (2019) 333–340

Contents lists available at ScienceDirect

Colloids and Surfaces B: Biointerfaces

journal homepage: www.elsevier.com/locate/colsurfb

Colorimetric detection of single base-pair mismatches based on the interactions of PNA and PNA/DNA complexes with unmodified gold nanoparticles

Shu Xing[a,1], Xiaojun Xu[a,c,1], Pan Fu[a,b], Mengjia Xu[a,b], Tingting Gao[a], Xiaokang Zhang[a], Chao Zhao[a,*]

[a] Cixi Institute of Biomedical Engineering, Ningbo Institute of Materials Technology and Engineering, Chinese Academy of Sciences, Ningbo 315201, PR China
[b] University of Chinese Academy of Sciences, Beijing 100049, PR China
[c] Institute of Pharmaceutical Chemistry, Zhejiang Pharmaceutical College, Ningbo 315100, PR China

ARTICLE INFO

Keywords:
Single base-pair mismatch discrimination
Peptide nucleic acids
Gold nanoparticles
Nucleases
Colorimetric assay

ABSTRACT

Rapid and sensitive single nucleotide polymorphisms (SNPs) genotyping is of particular important for early diagnosis, prevention, and treatment of specific human diseases. A simple and low-cost SNP detection method would be valuable for routine analysis in resource-limited settings. Here, we demonstrated a novel and convenient gold nanoparticle (AuNPs) based colorimetric approach for efficient screening of SNPs at room temperature without instrumentation. SNP detection is performed in a single tube with one set of unmodified AuNPs, a label-free peptide nucleic acid (PNA) probe, a single exonuclease (S1 nuclease), and the target to be tested. S1 nuclease could digest DNAs in DNA/PNA duplexes involving a mismatch into small fragments, while DNAs in the fully-matched DNA/PNA duplexes can be effectively protected by PNA from enzymatic degradation. This difference could be easily discriminated by color changes associated with gold aggregation. PNA oligomers can induce immediate AuNP aggregation even in the presence of nucleoside monophosphates (dNMPs), the digestion products of DNA. Whereas PNA/DNA duplexes can effectively stabilize unmodified AuNPs, and the stabilization effect of PNA/DNA is better than single-stranded DNA (ssDNA) and double-stranded DNA (dsDNA). Without the need of precise temperature control and extra salt addition, SNPs are detected with a detection limit of 2.3 nM in cell lysate. Moreover, this system can effectively discriminate a range of different mismatches even in spiked cell lysate, demonstrate the potential use of this biosensor for biological samples.

1. Introduction

Single nucleotide polymorphisms (SNPs), the most common form of genetic variation present among individuals, occur as frequently as every few hundred to few thousand base pairs in the human genome [1] and information from SNPs is of great importance for heredity-related risk assessment, early diagnosis, drug discovery, forensics, agriculture and so on [2]. Currently, numerous SNP detection methods have been developed, including traditional gel electrophoresis-based methods [3], sequencing [4], microarray technology [5], mass spectrometry [6], TaqMan assays [7] and methods using enzymatic reactions [8]. However, these approaches suffer from low sensitivity or poor specificity at room temperature and effective SNP discrimination usually requires the use of specialized equipment, trained personnel or high-stringency conditions with precise temperature control. Additionally, the time, expense and complexity of these methods are of impractical for small hospitals or developing world settings. Therefore, a method which fulfills versatile requirements (cheapness, easiness, promptness, preciseness, room-temperature assays and others) would be valuable for routine analysis in resource-limited settings.

Gold nanoparticles (AuNPs) are widely used for chemical and biological detection [9] because of their high extinction coefficients [10], strong size- and distance-dependent optical properties [11], high quenching efficiency toward various fluorophores [12], easy immobilization of various functional molecules [13], or their capability of further amplification by silver stain [14]. AuNPs-based colorimetric SNP detection methods have attracted a lot of attention due to their visibility and low-cost. The response of AuNPs to light is strongly

* Corresponding author.
E-mail address: zhaochao@nimte.ac.cn (C. Zhao).
[1] S.X. and X.X. contributed equally to this work.

https://doi.org/10.1016/j.colsurfb.2019.05.069
Received 8 February 2019; Received in revised form 22 May 2019; Accepted 27 May 2019
Available online 28 May 2019

influenced by their environment, size and physical dimensions. The resulting color change would be so distinct that it is readily visible to the eye by changing size, shape, interparticle plasmon coupling, surface chemistry or aggregation state of AuNPs [15]. Mirkin and his colleagues were the first to report an AuNP-based SNP detection strategy, which relies on hybridization-driven AuNP aggregation. In this assay, two sets of DNA-modified AuNPs were cross-linked via target hybridization, and a single-base mismatch was directly observed on a C18 thin-layer chromatography plate at 58 °C [11]. To improve the sensitivity and/or specificity, subsequently developed AuNP-based SNP detection platforms involved target recycling or target amplification by the use of ligation reaction [16,17], nicking endonucleases [18], primer extension reaction [19], rolling circle amplification [20] and so on. For example, Xiao and his colleagues reported an Exo III-assisted target recycling SNP detection method. In this assay, thiolated DNA containing two abasic site were specially designed. Apurinic endonucleolytic activity of Exo III at mismatched site was significantly inhibited and solution remained red due to insufficient shear of DNA on AuNPs surface. In contrast, for perfectly matched target, AuNPs were stepwise sheared to change blue in high-salt buffer and target was released to start a new cycle [21]. However, these methods as described above need labeled probes and time consuming preparation of modified AuNPs (20–40 h of assembly). To overcome these shortcomings, label-free detection methods that uses unmodified probes and unmodified AuNPs have been developed [22,23]. These method is based on the finding that the adsorption of ssDNA on unmodified AuNPs could effectively stabilize the colloid against salt-induced aggregation, but the precise temperature control and the relatively poor specificity and detection limits were still critical for the method. To improve the specificity of the unmodified-AuNP based methods for single-base mismatch detections, a label-free colorimetric assay for single-base mismatches has been reported by the combination of unmodified AuNPs and structure-selective nucleases [24]. The method is based on the stabilization effect of dNMPs to unmodified AuNPs, which is better than ssDNA and dsDNA, and the high mismatch discrimination capability of nucleases. It eliminates the need of target modification, precise temperature control or stringent washes. However, the use of biodegradable DNA probe and extra steps of salt addition make it inconvenient to carry and complicated to operate.

Peptide nucleic acids (PNAs) are man-made DNA/RNA analogues in which the entire sugar-phosphate backbone is replaced by a neutral polyamide backbone [25]. Distinct backbone properties (uncharged, high rigidity, non-nature) endow PNA with exceptional chemical, physical and biological properties such as higher binding affinity, better specificity and excellent biological stability, which enables PNA to be an important supplement of DNA in many applications [26–32]. For example, PNA could induce immediate aggregation of citrate ion-coated AuNPs and silver nanoparticles (AgNPs), while PNA/DNA complexes can effectively protect the particles from salt induced aggregation [33]. By taking advantage of this property, Su and his colleagues reported a colorimetric method for DNA detection [34]. Moreover, the hybridization of PNA with a complementary RNA could also disrupt the PNA-induced metallic nanoparticle aggregation, which is used to construct colorimetric assays for the detection and quantification of RNAs [35–37]. Given this and the limitations of the above mentioned SNP detection methods, a label-free method using PNA and unmodified AuNPs for rapid and specific assaying nucleic acids is still attractive and necessary. However, until now, there is no such a method reported, even though it is important.

Herein we present a simple platform that enables rapid, label-free, naked-eye detection of SNPs with minimal reagent and equipment requirements at room temperature. SNP detection is performed in a single tube with one set of unmodified AuNPs, a label-free PNA probe, a single exonuclease (S1 nuclease), and the target to be tested. We demonstrated that this proposed method was highly effective for the detection of single-base mismatches, without the need of precise temperature control and extra salt addition, as well as other inherited advantages of label-free AuNP-based colorimetric assays.

2. Experimental section

2.1. Materials and reagents

Fmoc protected PNA monomers were purchased from PANAGENE Inc. (Korea). Methyl-benzhydrylamine (MBHA) resin was purchased from CSBio Ltd (USA). The PNAs were manually prepared by the solid-phase peptide synthesis method as we reported previously [28]. The PNAs were purified by a reverse-phase HPLC column (Agilent Eclipse XDB-C18) and verified by mass analysis (see Fig. S1). The concentration of PNAs was measured at 260 nm. DNA oligonucleotides were synthesized and purified by Jie Li Biology Inc. (China). All PNA and DNA sequences used in this study were listed in Electronic Supplementary material Table S1. $HAuCl_4{\cdot}3H_2O$ (99.9%), $AgNO_3$ (99.8%), trisodium citrate dihydrate (99.5%), and $NaBH_4$ (98%) were purchased from Sinopharm Chemical Reagent Co. Ltd. (Shanghai, China). S1 enzyme was purchased from Thermo Fisher Scientific Inc. (USA) and the nuclease was stored on ice prior to use. Human non-small cell lung cancer (NCI-H1299) cell was purchased from the cell bank of the Chinese Academy of Sciences (Shanghai, China). The RPMI 1640 medium and FBS were purchased from Thermo Scientific (USA). RIPA lysis buffer was purchased from Beyotime Biotech (China). All other regents were purchased from Aladdin (China). Ultrapure water (18 MΩ) was generated from a Millipore (Merck) Milli-Q water system.

2.2. Preparation of gold and silver nanoparticles

Citrate-stabilized AuNPs were prepared by thermal reduction of $HAuCl_4$ with sodium citrate. Citrate-stabilized AgNPs were synthesized by the reduction of silver nitrate using sodium borohydride. Prior to nanoparticles preparation, all glassware was thoroughly cleaned with freshly prepared aquaregia (3:1 HCl/HNO_3). The quality of the particles was monitored using UV–vis spectrophotometer and transmission electron micrographs (TEM) (Fig. S2). The concentrations of the AuNPs [38] and AgNPs [39,40] were calculated according to Beer's laws using their extinction coefficients. The solution was stored at 4 °C before use.

2.2.1. Preparation of AuNPs

Citrate-stabilized AuNPs with a diameter of ~13 nm were prepared using a standard protocol [41]. Briefly, 50 ml $HAuCl_4$ solution (1 mM) was heated with continuous stirring until the solution started boiling and refluxed for 10 min. Then, 5 ml trisodium citrate solution (38.8 mM) was quickly added to the boiling solution. The solution was kept boiling and stirred for an additional 15 min after a brick-red wine color appeared. Then, the boiling was stopped and the solution was slowly cooled down to room temperature. In addition, AuNPs with a diameter of 25 ± 3 nm were also synthesized by this method with the use of 50 mL of 0.25 mM $HAuCl_4$ and 1.5 mL of 38.8 mM trisodium citrate.

2.2.2. Preparation of AgNPs

Citrate-stabilized AgNPs with a diameter of ~16 nm were prepared via a previously reported method [42]. Briefly, 125 μL of 100 mM $AgNO_3$ and 125 μL of 100 mM trisodium citrate were added into 50 mL of water under stirring. Then 3 mL of freshly prepared 5 mM $NaBH_4$ was added into the above aqueous solution under vigorous stirring. The resulting yellow colloidal silver solution was further stirred for 30 min and then was left undisturbed overnight.

2.3. Detection of single-base mismatches using S1 nuclease

PNA (8.33 μM) and equimolar fully-matched DNA target or single-base mismatched targets were mixed in 6 μL buffer solution containing 20 mM NaCl buffer. The mixture was kept at room temperature for

10 min, followed by adding 1 μL of solution containing 80 mM CH_3CO_2Na, 600 mM NaCl, and 4 mM $ZnSO_4$, pH 4.6 and 1 μL of solution containing various concentrations of S1 nuclease. The mixture was incubated at 25 °C for a predetermined time. After enzymatic digestion the reaction products were immediately mixed with 42 μL of AuNP or AgNP solution (10 nM). Photographs were taken by use of a digital camera after 15 min ~ 1 h following adding AuNPs or AgNPs solution. UV/vis absorption spectra were recorded using an Agilent (USA) Cary 300 Bio UV/vis spectrophotometer or a Molecular Devices (USA) SpectraMax 190 microplate reader. Similar protocol was performed for the single-base mismatch detection of targets in NCI-H1299 cell lysate.

To validate this SNPs assay, single-base mismatch detection was also performed by using a same sequence DNA probe instead of the PNA probe under the same conditions as described previously [24].

2.4. Preparation of cell lysate

NCI-H1299 cells were trypsinized and collected by centrifugation at 2400 rpm for 5 min at 4 °C, the supernatant was discarded and the cells were washed with PBS buffer. Then the cells were centrifuged again to remove the supernatant at 2400 rpm for 5 min at 4 °C. After centrifugation, the cells were suspended in RIPA lysis buffer at a concentration of 10^6 cell/mL and kept on ice for 40 min. Finally, the lysis products were centrifuged at 12,000 rpm for 30 min at 4 °C, the supernatant was collected and stored in −20 °C. To prepare the cell lysate samples, PNA/fully-matched or single-base mismatched target complexes were diluted in 10% NCI-H1299 cell lysate for SNPs detection.

2.5. Gel electrophoresis

PNA (8.33 μM) and equimolar fully-matched DNA target (FM) or single base-mismatched DNA target (1 MM) were mixed in 6 μL buffer solution containing 20 mM NaCl buffer. The mixture was kept at room temperature for 10 min, followed by adding 1 μL of solution containing 80 mM CH_3COONa, 600 mM NaCl, and 4 mM $ZnSO_4$, pH 4.6 and 1 μL of solution containing 5.6 U/μL S1 nuclease. The mixture was incubated at 25 °C for 30 min. After enzymatic digestion the reaction products were run on a 10% polyacrylamide gel under denaturing conditions and stained with GelRed for 15–30 min. The gel was imaged for further analysis using a Tanon 2500 imaging system.

3. Results and discussion

3.1. Assay principle

The principle of the proposed single-base mismatch detection method is illustrated in Scheme 1. A 15-base PNA probe, which is used to recognize target DNA, was designed and synthesized by the method of solid-phase peptide synthesis as described previously [28]. In a typical sensing process, target DNA is first hybridized with the probe PNA followed by the S1 nuclease digestion. S1 nuclease is a commonly used single strand-specific nuclease, which could digest all unhybridized ssDNA, overlapping ssDNA segments that extend beyond the region of the PNA/DNA duplex, and any unbound mismatches within a duplex [43–47]. So in this sensing system, if probe PNA is perfectly complementary to the target DNA, complementary DNA sequence of target DNA will be protected by PNA from the digestion by nuclease S1 (see Electronic Supplementary material Fig. S3, Lane 2). In contrast, the DNA substrates, contain a mismatch toward probe PNA, will be completely digested down to mononucleotides under identical conditions (see Electronic Supplementary material Fig. S3, Lane 3). The remarkable discrimination between matching site and mismatching site by the PNA/nuclease S1 combinations could be easily monitored by the specific color changes associated with gold aggregation. It has been reported that PNA oligomers can induce immediate particle aggregation by shielding the citrate ions on the surface of AuNPs [33]. Our study further proved that PNA could induce AuNP aggregation even in the presence of nucleoside monophosphates (dNMPs), the digestion products of DNA (see Electronic Supplementary material Fig. S4). While PNA/DNA complex, although having a stable double helix structure similar to dsDNA, can effectively protect AuNPs from salt induced aggregation (see Electronic Supplementary material Fig. S5), and the ability of PNA/DNA to protect AuNPs against salt-induced aggregation is stronger than ssDNA [33]. This is caused by the larger molecular size and the structure rigidity of PNA/DNA complex that introduces more steric protection than ssDNA [33].

As shown in Scheme 1, AuNPs were protected by the fully-matched PNA/DNA duplexes, solutions of AuNPs remain red in the presence of PNA/DNA. When there is a mismatch in the target DNA toward probe PNA, the target DNA will be cleaved by S1 nuclease into small fragments, the relatively high coating efficiency of PNA lead immediate coagulation of AuNPs and the solution changes from red to purple-blue. Thus the discrimination between matching site and mismatching site by the PNA/nuclease S1 can be easily screened with naked eye based on the specific color changes.

3.2. Verification of the discrimination capability

Fig. 1 shows the color and UV/Vis absorption spectra changes of AuNP solutions before and after addition of different PNA/DNA complexes after S1 nuclease digestion. Without PNA/DNA complexes, the solution of AuNP is red and has a plasmon absorption peak at 520 nm (Blank). After addition of the fully-matched PNA/DNA complexes, the absorbance intensity at 520 nm increased slightly and the peak position redshifted to 523 nm, and the solution color slightly changed to dark red (FM), indicating that the formation of PNA/DNA duplex after S1 nuclease digestion, which can effectively protect the particles from salt induced aggregation. However, when the single-base mismatched PNA/DNA complexes were presented, the solution color changed from red to purple-blue (1 MM), indicating that the cleavage of the mutant DNA by

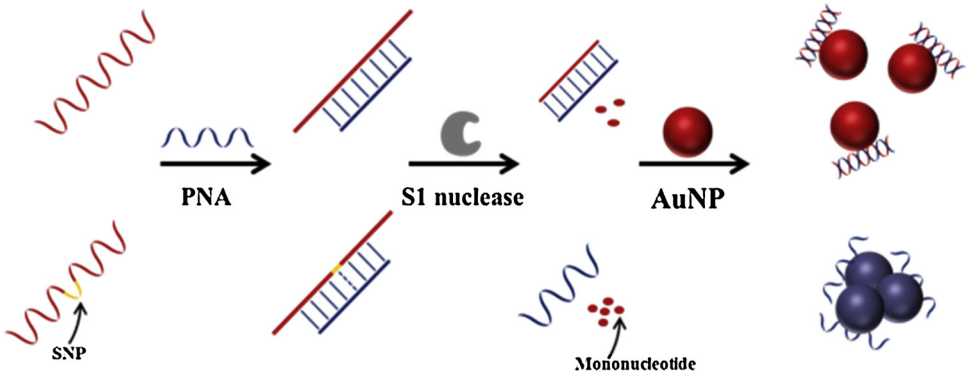

Scheme 1. Schematic illustration of the optical detection of single-base mismatches.

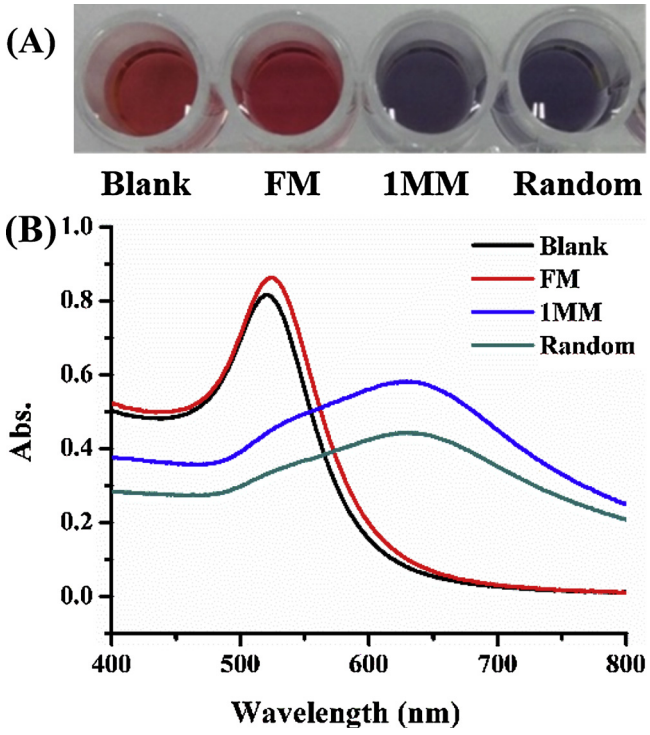

Fig. 1. (A) Photographs and (B) UV/vis absorption spectra of AuNP solutions in the absence (blank) and presence of fully matched PNA/DNA complexes (FM, PNA/C-G, see Electronic Supplementary material Table S1), PNA/DNA complexes that containing a mismatch in the target DNA toward probe PNA (1 MM, PNA/C-A-1, see Electronic Supplementary material Table S1), and a mixture of a random sequence DNA and the probe PNA (Random, see Electronic Supplementary material Table S1) after S1 nuclease digestion. The concentration of AuNPs, PNA and target DNAs are 10 nM, 1.0 μM, and 1.0 μM, respectively.

S1 nuclease and the released PNA induced the aggregation of AuNPs. This is further confirmed by the disappearance of the absorption peak at 520 nm and a distinct increase of absorption at 625 nm in the UV–vis absorption spectra. These observations clearly demonstrate the feasibility of the proposed method to detect single-base mismatches.

3.3. Optimum conditions for the SNP sensor

As we know, the amount of S1 nuclease and the enzymatic digestion time strongly affects the recognition specificity of S1 to its substrate. To achieve the optimal discrimination capability against single-base mismatches, cleavage reactions with various concentrations of S1 nuclease at different time points were performed, and the absorption intensities of the resulting AuNP solutions at 520 nm and 610 nm were recorded by a microplate reader, respectively. In order to quantitatively measure the discrimination capability of our SNP detection method, the single-base mismatch discrimination factor (DF) was defined as the ratio of A_{610nm}/A_{520nm} of single-base mismatched target to that of fully-matched target. A larger DF is indicative of better specificity. As shown in Fig. 2A, keeping the digestion time at 30 min, the DF was gradually increased from one plateau period to another as the concentration of S1 nuclease increased from 0.1 U/μL to 0.8 U/μL, and the maximum DF value of 7.5 was achieved at the S1 concentration of 0.7 U/μL. Similarly, to obtain optimized digestion time of S1 nuclease, cleavage reactions at different time points from 10 min to 60 min were conducted. The DF increased with the increase of the reaction time from 10 min to 30 min. However, with further increase in the reaction time, the DF decreased. The biggest DF value of 7.5 was achieved after 30 min at the S1 concentration of 0.7 U/μL (Fig. 2B). Therefore, to get the highest discrimination capability

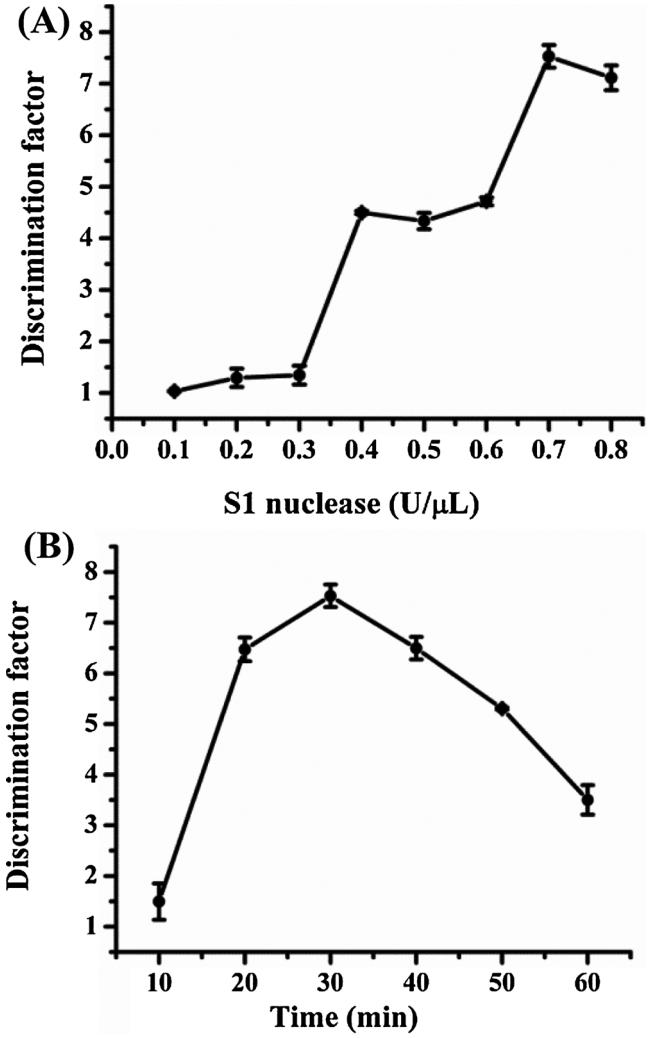

Fig. 2. (A) The effect of S1 nuclease concentration on discrimination factors of the SNP sensor. Each assay was incubated for 30 min at 25 °C. (B) The effect of S1 nuclease digestion time on discrimination factors of the SNP sensor. Each assay contained 0.7 U/μL of S1 nuclease and incubated at 25 °C. Error bars estimated as the standard deviation of three replicates.

of the sensor for SNPs, the S1 nuclease concentration of 0.7 U/μL and the digestion time of 30 min were used in the following experiments.

3.4. Specificity of the SNP sensor

As demonstrated above, our SNP detection system was capable of discriminating between C-A mismatched target and perfectly complementary DNA (Fig. 1). To evaluate the general applicability of the proposed method for other SNP types, 60-base long fully-matched and single-base mismatched targets were designed, and all 8 types of base-pair mismatches and 8 types of different positions (Table 1) across the middle sequence of the target were investigated using our method. The detection results were listed in Table 1 and shown in Fig. 3.

For all single-base mismatched targets, the DF values were in the range of 2.19 ± 0.13 to 7.89 ± 0.19. The detection system has the highest discrimination capability towards duplexes containing a C/C mismatch, whereas the lowest was observed for the duplexes with a T/G mismatch. This result was consistent with previous findings that the thermodynamics of mismatches depend on the identity of the mismatched base pair as well as the identity of its near neighbors [48,49]. Another interesting phenomenon is that higher DF values were obtained for the duplexes that contain a mismatch located near the middle

Table 1
Discrimination factors of the SNP sensor for various single-base mismatched targets (1 MM, mismatched bases are marked in bold and underscore), (SD, n = 3).

Name	Mismatched base-pairs	DNA target sequence (5' → 3')	Discrimination factors
C-A-1	C-A	22mer-TGAGTGT**A**TAACGGA-23mer	7.53 ± 0.22
A-A	A-A	22mer-TGAGTGTG**A**AACGGA-23mer	4.32 ± 0.56
T-T	T-T	22mer-TGAGTGTG**T**TACGGA-23mer	4.00 ± 0.58
T-C	T-C	22mer-TGAGTGTGTA**C**CGGA-23mer	4.12 ± 0.62
G-A	G-A	22mer-TGAGTGTGTAA**A**GGA-23mer	7.27 ± 0.24
C-C	C-C	22mer-TGAGTGTGTAAC**C**GA-23mer	7.89 ± 0.19
C-A-2	C-A	22mer-TGAGTGTGTAACG**A**A-23mer	3.36 ± 0.43
T-G	T-G	22mer-TGAGTGTGTAACGG**G**-23mer	2.19 ± 0.13
G-G	G-G	22mer-TGAGTGTGTAA**G**GGA-23mer	3.21 ± 0.28

of the target (Fig. 3A). So, it is possible to us to get a rough idea about the mutation type and the mutation position of the target based on these observations. Furthermore, the strict discriminations between fully-matched and mismatched targets could also be easily visualized to naked eyes using our method based on the color change of the AuNP solutions. As the aggregation degree increased, the color of the AuNP solution changes from red to purplish red, purple, blue, grey and colorless at the end when AuNPs precipitate out of the solution completely. Fig. 3B showed clearly that only the solution of AuNPs containing the perfect matched DNA target is red. The others containing single-base mismatched targets turns purple or blue that could be easily distinguished from the perfect matched ones with naked eyes. The apparent color change for different mutation types could be further confirmed by the different red-shifting degree of the absorption peak of AuNPs in the UV–vis absorption spectra (Fig. 3C). These results demonstrate that the proposed SNP sensor is able to effectively discriminate a range of mismatched DNA targets from the fully matched ones.

3.5. Validation of the SNP sensor

To validate the advantages of the PNA probe based SNP sensor, the analytical performance of the well-established DNA probe based SNP discrimination method was also done by using the same sequence DNA

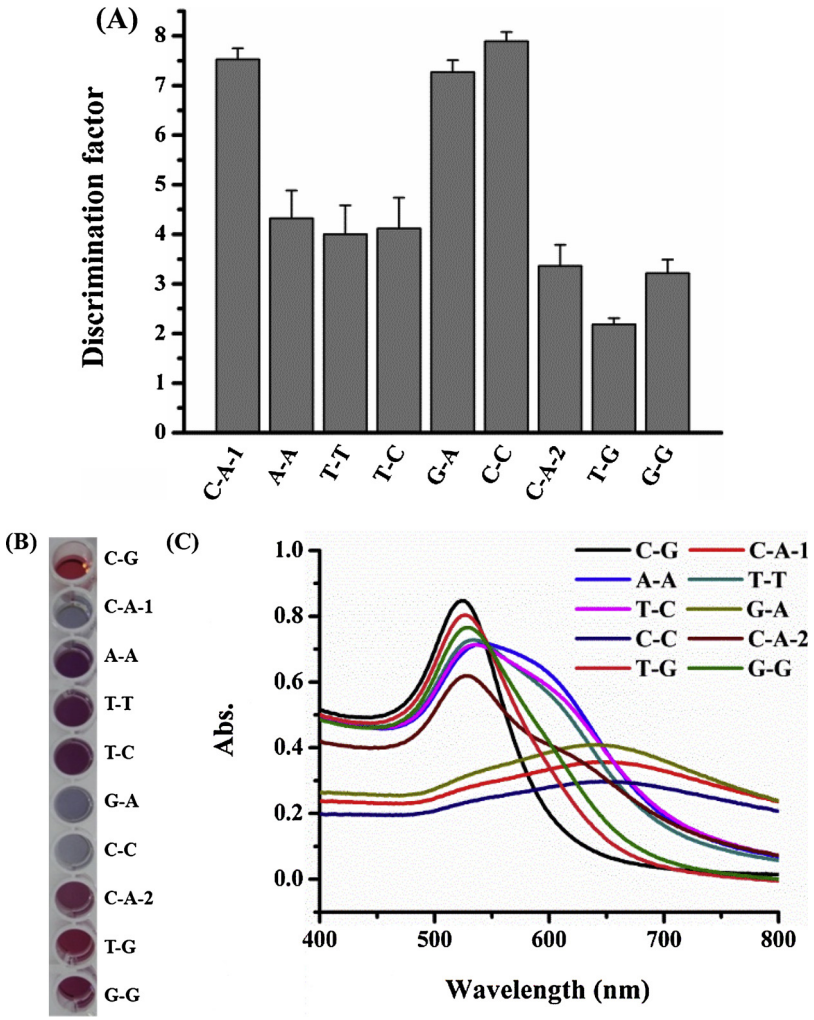

Fig. 3. (A) Comparison of the discrimination factors of the SNP sensor for various single-base mismatched targets. (B) Photographs and (C) UV/vis absorption spectra of AuNP solutions in the presence of fully-matched PNA/C-G complexes and various PNA/single-base mismatched targets after S1 nuclease digestion. The concentration of AuNPs, PNA and target DNAs are 10 nM, 1.0 μM, and 1.0 μM, respectively. Error bars estimated as the standard deviation of three replicates.

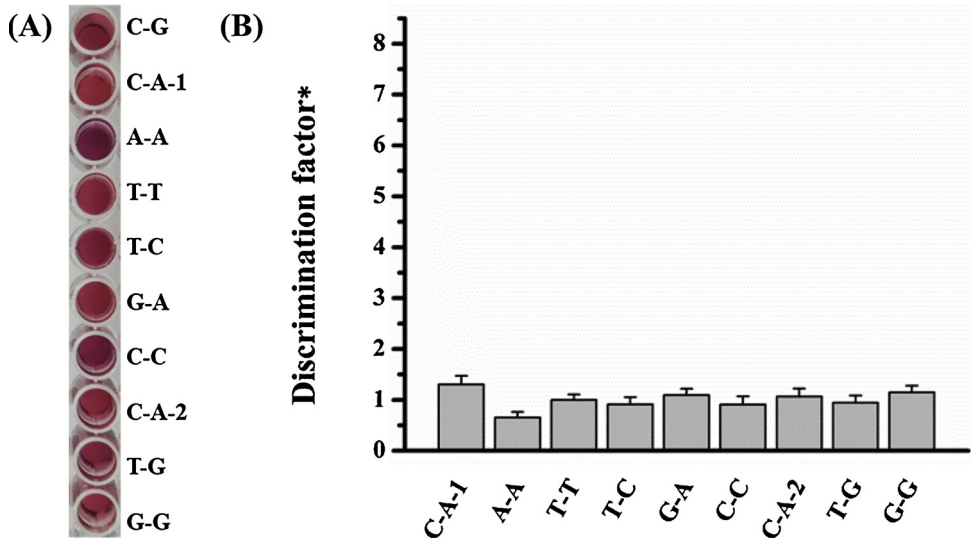

Fig. 4. (A) Photographs and (B) Discrimination factors of the DNA probe based SNP sensor for various single-base mismatched targets. The concentration of AuNPs, DNA probe and target DNAs are 10 nM, 1.0 μM, and 1.0 μM, respectively. Error bars estimated as the standard deviation of three replicates.

probe instead of the PNA under the same conditions as described previously [24]. As shown in Fig. 4, the DF values, which was defined as the ratio of A_{610nm}/A_{520nm} of fully-matched target to that of single-base mismatched target, for all single-base mismatched targets were less than 1.5, and no apparent color change (from red to purple-blue) was observed for the resulting AuNP solutions, indicating the weak discrimination capability for single-base mismatches of the DNA probe based SNP sensor. These results further confirmed that the use of the PNA probe instead of DNA could enhance the single-base mismatch discrimination capability of the AuNP/S1 nuclease based SNP sensor. In addition, the higher stability towards the degradation of nucleases and proteases and the higher thermal stability and sequence selectivity make PNA an idea candidate for SNP screening in real complicated environment.

3.6. Sensitivity of the SNP sensor

To test the sensitivity of the assay, the sensor solution were treated with different concentrations of single-base mismatched DNA target and the absorbance signals at 610 nm (A_{610nm}) and 520 nm (A_{520nm}) were recorded. As a negative control, different concentrations of fully-matched DNA target were also tested under the same conditions. As indicated in Fig. 5, the ratio of A_{610nm}/A_{520nm} is sensitive to the single-base mismatched target and increases as the concentration of target C-A-1 DNA increases. This increase is attributed to the digestion of the DNAs in the single-base mismatched PNA/DNA complexes, and resulting in the releasing of PNAs, which will lead the coagulation of AuNPs in solution. While for the fully matched DNAs, the increase in the amount of fully-matched PNA/DNA complexes has minor influence on the aggregation state of AuNPs, so the A_{610nm}/A_{520nm} remain virtually unchanged. A linear correlation exists between A_{610nm}/A_{520nm} and the concentration of the C-A-1 DNA target over the range of 50–200 nM (blue line). This sensor has a detection limit of 6.1 nM, based on 3σ/slope (where σ is the standard deviation). These data show high sensitivity and good linearity for the quantitative analysis of SNPs by using the PNA-AuNP sensor. In addition, this SNP sensor has a visual detection limit of 60 nM (see Electronic Supplementary material Fig. S6), which could be recognized with naked eyes based on the color change of AuNPs. Although the detection sensitivity is lower than that of the surface plasmon resonance (SPR) based method [50], the visual detection limit and the dynamic range of the SNP sensor are comparable to those of other AuNP-based DNA detection methods [11,24].

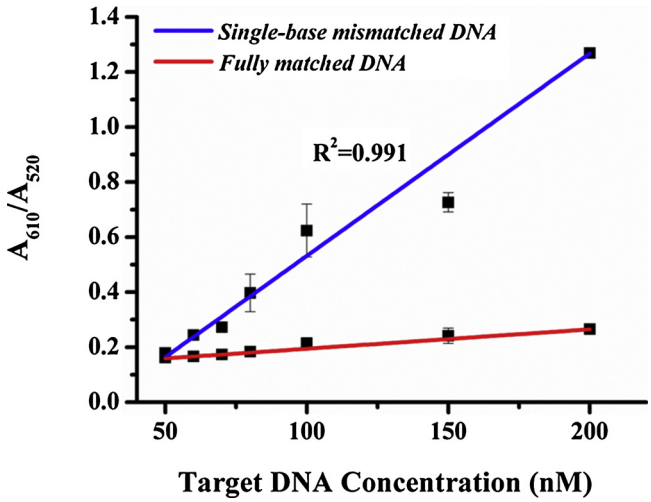

Fig. 5. Linear relationship between A_{610nm}/A_{520nm} and the concentration of single-base mismatched DNA target (C-A-1, blue line). As a negative control, the fully matched DNA target (C–G) is also included. Error bars estimated as the standard deviation of three replicates (For interpretation of the references to colour in this figure legend, the reader is referred to the web version of this article.).

3.7. Detection of SNPs in spiked sample

To evaluate the feasibility of the SNP sensor for real samples, the analysis of target DNAs in NCI-H1299 cell lysate was conducted by the developed SNP assay. Tests were performed by adding various concentrations (10, 20, 30, 40 and 50 nM) of fully-matched target or single-base mismatched target (C-A-1 DNA) to 10% NCI-H1299 cell lysate. The cell lysate alone cannot cause apparent aggregation of AuNPs (see electronic supplementary material Fig. S7), however, with the addition of the single-base mismatched DNA target, the ratio of A_{610nm}/A_{520nm} increased linearly over the concentration range of 10–50 nM (Fig. 6). While for the fully matched DNAs, the A_{610nm}/A_{520nm} changed slightly. The calculated detection limit for the single-base mismatched target in 10% cell lysate is 2.3 nM and the visual detection limit is 20 nM (see electronic supplementary material Fig. S8), which is comparable or even better than that in buffer, indicating the possibility of applying this sensing strategy for SNPs detection in biological samples.

Furthermore, the recovery assays were also performed by spiking

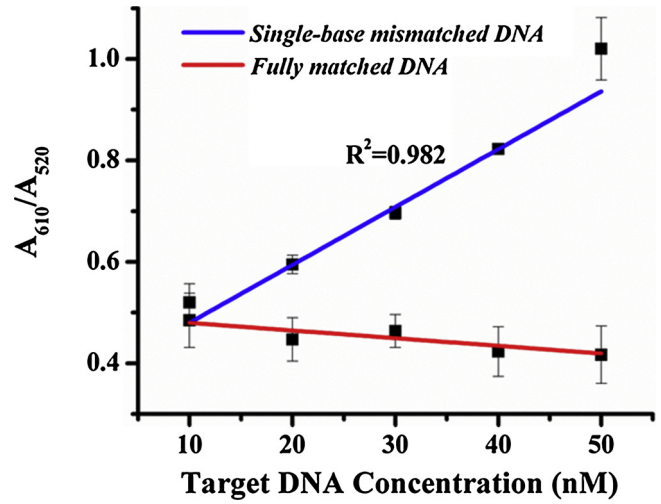

Fig. 6. Linear relationship between A_{610nm}/A_{520nm} and the concentration of single-base mismatched DNA target (C-A-1, blue line) in 10% NCI-H1299 cell lysate. As a negative control, the fully matched DNA target (C–G) is also included. Error bars estimated as the standard deviation of three replicates (For interpretation of the references to colour in this figure legend, the reader is referred to the web version of this article.).

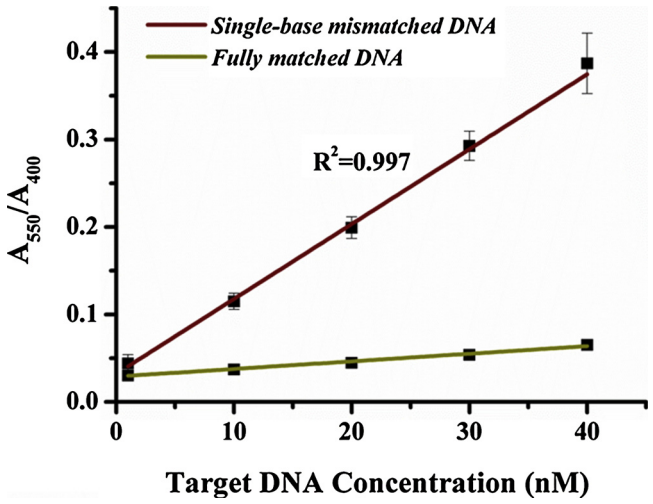

Fig. 7. Linear relationship between A_{550nm}/A_{400nm} and the concentration of single-base mismatched DNA target (C-A-1). As a negative control, the fully matched DNA target (C–G) is also included. Error bars estimated as the standard deviation of three replicates.

Table 2
Recovery of the single-base mismatched target (C-A-1) in 10% cell lysate samples obtained with the proposed SNP sensor (n = 4).

Name	Added Target (nM)	Found (nM)	Recovery (%)	SD (n = 4)
1	15.0	14.4	96	1.8
2	60.0	60.9	101.5	1.6
3	80.0	81.6	102	0.4

the single-base mismatched target (C-A-1: 15 nM, 60 nM, and 80 nM) into 10% cell lysate samples. Acceptable recoveries (between 96% and 102%) and standard deviations (between 0.4 and 1.8) were obtained (Table 2), indicating that the developed SNP sensing strategy could be applied to quantify the concentration of the single-base matched target in real biological samples.

3.8. Colorimetric detection of single-base mismatches using AgNPs or larger size AuNPs

To get an optimum sensitivity of the colorimetric assay for single-base mismatches, AgNPs of 16 nm in diameter (Fig. S2), which is the most commonly used particle size in nucleic acid adsorption studies and in bioassays, were also used to develop the robust colorimetric strategy. As displayed in Fig. S9, PNA could induce immediate AgNPs aggregation without the help of salt, and the color of AgNPs solution changed from yellow to brown. The drop of absorbance at the surface plasmon peak (~400 nm) and the appearance of surface plasma peak at longer wavelength (~550 nm) further confirmed the particle aggregation (Fig. S9B). However, the hybridization of PNA with DNA disrupt the PNA-induced aggregation, and PNA/DNA complexes could even protect AgNPs from salt-induced aggregation (Fig. S9A). Therefore, AgNPs could be an alternative of AuNPs for colorimetric SNP detection. To determine the sensitivity of the AgNPs-based method, the absorbance at 550 nm and 400 nm were recorded at different concentrations of single-base mismatched DNA target. The ratio of A_{550nm}/A_{400nm} increases linearly over the concentration range from 1 nM to 40 nM (Fig. 7). This sensor has a calculated detection limit of 0.95 nM and a visual detection limit of 10 nM (Fig. S10) for the single-base mismatched DNA target, which is superior to that of AuNPs-based method, indicating that AgNPs is a more sensitive colorimetric platform for single-base mismatch detection. In addition to AgNPs, larger size AuNPs (25 nm) were also used to develop the colorimetric assay. Similar results were obtained as that of 13 nm AuNPs (Fig. S11), indicating the feasibility of using larger size AuNPs to develop colorimetric assays to detect single-base mismatches. But in consideration of the complexity, stability and the cost in preparation of AgNPs and larger size AuNPs, the commonly used 13 nm AuNPs are still our first choice.

4. Conclusions

In summary, we have demonstrated a simple, rapid, label-free, and sensitive colorimetric method for efficient screening of single base-pair mismatches based on the different binding affinities of AuNPs to single-stranded PNA and PNA/DNA duplexes. This sensor displayed high discrimination capability to single-base mismatched DNAs against fully-matched target DNA sequence. This strategy has several excellent features. First, the use of unmodified AuNPs and label-free PNA probes offers a convenient colorimetric “mix-and-detect” approach for the rapid detection of SNPs at room temperature. It eliminates the need of time consuming preparation of labeled substrates and AuNPs, the requirements for stringent temperature control and multiple steps of post-washes, and any complicated instruments. Second, the use of a sequence-specific PNA probe impart high sensitivity and selectivity to the sensor. Third, the use of a 60-base long target provides the potential for detection of a DNA fragment which can be extracted through the DNA amplification protocol, for example, the real-time polymerase chain reaction amplification, in real sample. Finally, this assay in principle can be used to detect any kind of gene mutations by simply changing the PNA sequences that selectively bind to other gene targets. Furthermore, the use of PNA probe makes this sensing platform a promising approach for the analysis of SNPs at point-of-care in resource-limited settings.

Conflict of interest

The authors declare that they have no conflict of interest.

Acknowledgements

This work was supported by Ningbo Natural Science Foundation (2017C110020, 2018A610318), China Postdoctoral Science Foundation (2017M621982), Zhejiang Postdoctoral Research Projects Preferred

Funding, and funds from Ningbo Institute of Materials Technology and Engineering, Chinese Academy of Sciences.

Appendix A. Supplementary data

Supplementary material related to this article can be found, in the online version, at doi:https://doi.org/10.1016/j.colsurfb.2019.05.069.

References

[1] D.G. Wang, J.B. Fan, C.J. Siao, A. Berno, P. Young, R. Sapolsky, G. Ghandour, N. Perkins, E. Winchester, J. Spencer, L. Kruglyak, L. Stein, L. Hsie, T. Topaloglou, E. Hubbell, E. Robinson, M. Mittmann, M.S. Morris, N. Shen, D. Kilburn, J. Rioux, C. Nusbaum, S. Rozen, T.J. Hudson, R. Lipshutz, M. Chee, E.S. Lander, Large-scale identification, mapping, and genotyping of single-nucleotide polymorphisms in the human genome, Science 280 (1998) 1077–1082.

[2] A.J. Brookes, The essence of SNPs, Gene 234 (1999) 177–186.

[3] A.C. Syvänen, From gels to chips: "minisequencing" primer extension for analysis of point mutations and single nucleotide polymorphisms, Hum. Mutat. 13 (1999) 1–10.

[4] H. Fakhrai-Rad, N. Pourmand, M. Ronaghi, Pyrosequencing: an accurate detection platform for single nucleotide polymorphisms, Hum. Mutat. 19 (2002) 479–485.

[5] H. Matsuzaki, S. Dong, H. Loi, X. Di, G. Liu, E. Hubbell, J. Law, T. Berntsen, M. Chadha, H. Hui, G. Yang, G.C. Kennedy, T.A. Webster, S. Cawley, P.S. Walsh, K.W. Jones, S.P.A. Fodor, R. Mei, Genotyping over 100,000 SNPs on a pair of oligonucleotide arrays, Nat. Methods 1 (2004) 109–111.

[6] J. Tost, I.G. Gut, Genotyping single nucleotide polymorphisms by mass spectrometry, Mass Spectrom. Rev. 21 (2002) 388–418.

[7] L.G. Lee, C.R. Connell, W. Bloch, Allelic discrimination by nick-translation PCR with fluorgenic probes, Nucleic Acids Res. 21 (1993) 3761–3766.

[8] X. Wang, X.H. Lou, Y. Wang, Q.C. Guo, Z. Fang, X.H. Zhong, H.J. Mao, Q.H. Jin, L. Wu, H. Zhao, J.L. Zhao, QDs-DNA nanosensor for the detection of hepatitis B virus DNA and the single-base mutants, Biosens. Bioelectron. 25 (2010) 1934–1940.

[9] H. Jans, Q. Huo, Gold nanoparticle-enabled biological and chemical detection and analysis, Chem. Soc. Rev. 41 (2012) 2849–2866.

[10] R. Wilson, The use of gold nanoparticles in diagnostics and detection, Chem. Soc. Rev. 37 (2008) 2028–2045.

[11] R. Elghanian, J.J. Storhoff, R.C. Mucic, R.L. Letsinger, C.A. Mirkin, Selective colorimetric detection of polynucleotides based on the distance-dependent optical properties of gold nanoparticles, Science 277 (1997) 1078–1081.

[12] B. Dubertret, M. Calame, A.J. Libchaber, Single-mismatch detection using gold-quenched fluorescent oligonucleotides, Nat. Biotechnol. 19 (2001) 365–370.

[13] S.P. Song, Y. Qin, Y. He, Q. Huang, C.H. Fan, H.Y. Chen, Functional nanoprobes for ultrasensitive detection of biomolecules, Chem. Soc. Rev. 39 (2010) 4234–4243.

[14] Y.P. Bao, M. Huber, T.F. Wei, S.S. Marla, J.J. Storhoff, U.R. Muller, SNP identification in unamplified human genomic DNA with gold nanoparticle probes, Nucleic Acids Res. 33 (2005) e15.

[15] M. Stewart, C.R. Anderton, L.B. Thompson, J. Maria, S.K. Gray, J.A. Rogers, R.G. Nuzzo, Nanostructured plasmonic sensors, Chem. Rev. 108 (2008) 494–521.

[16] J. Li, X. Chu, Y. Liu, J.H. Jiang, Z. He, Z. Zhang, G. Shen, R.Q. Yu, A colorimetric method for point mutation detection using high-fidelity DNA ligase, Nucleic Acids Res. 33 (2005) e168.

[17] W. Shen, H.M. Deng, Z.Q. Gao, Gold nanoparticle-enabled real-time ligation chain reaction for ultrasensitive detection of DNA, J. Am. Chem. Soc. 134 (2012) 14678–14681.

[18] W. Xu, X.J. Xue, T.H. Li, H.Q. Zeng, X.G. Liu, Ultrasensitive and selective colorimetric DNA detection by nicking endonuclease assisted nanoparticle amplification, Angew. Chem. Int. Ed. 48 (2009) 6849–6852.

[19] I.K. Litos, P.C. Ioannou, T.K. Christopoulos, J. Traeger-Synodinos, E. Kanavakis, Genotyping of single-nucleotide polymorphisms by primer extension reaction in a dry-reagent dipstick format, Anal. Chem. 79 (2007) 395–402.

[20] J.S. Li, T. Deng, X. Chu, R.H. Yang, J.H. Jiang, G.L. Shen, R.Q. Yu, Rolling circle amplification combined with gold nanoparticle aggregates for highly sensitive identification of single-nucleotide polymorphisms, Anal. Chem. 82 (2010) 2811–2816.

[21] S. Wu, P.P. Liang, H.X. Yu, X.W. Xu, Y. Liu, X.H. Lou, Y. Xiao, Amplified single base-pair mismatch detection via aggregation of exonuclease-sheared gold nanoparticles, Anal. Chem. 86 (2014) 3461–3467.

[22] H.X. Li, L. Rothberg, Colorimetric detection of DNA sequences based on electrostatic interactions with unmodified gold nanoparticles, Proc. Natl. Acad. Sci. U. S. A. 101 (2004) 14036–14039.

[23] H.X. Li, L.J. Rothberg, Label-free colorimetric detection of specific sequences in genomic DNA amplified by the polymerase chain reaction, J. Am. Chem. Soc. 126 (2004) 10958–10961.

[24] M.Y. Liu, M. Yuan, X.H. Lou, H.J. Mao, D.M. Zheng, R.X. Zou, N.L. Zou, X.R. Tang, J.L. Zhao, Label-free optical detection of single-base mismatches by the combination of nuclease and gold nanoparticles, Biosens. Bioelectron. 26 (2011) 4294–4300.

[25] M. Egholm, O. Buchardt, P.E. Nielsen, R.H. Berg, Peptide Nucleic Acids (PNA). Oligonucleotide analogues with an achiral peptide backbone, J. Am. Chem. Soc. 114 (1992) 1895–1897.

[26] A. Ray, B. Nordén, Peptide nucleic acid (PNA): its medical and biotechnical applications and promise for the future, FASEB J. 14 (2000) 1041–1060.

[27] F. Pellestor, P. Paulasova, The peptide nucleic acids (PNAs), powerful tools for molecular genetics and cytogenetics, Eur. J. Hum. Genet. 12 (2004) 694–700.

[28] C. Zhao, T. Hoppe, M.K.H.G. Setty, D. Murray, T.W. Chun, I. Hewlett, D.H. Appella, Quantification of plasma HIV RNA using chemically-engineered peptide nucleic acids, Nat. Commun. 5 (2014) 5079.

[29] J.C. Wu, Q.C. Meng, H.M. Ren, H.T. Wang, J. Wu, Q. Wang, Recent advances in peptide nucleic acid for cancer bionanotechnology, Acta Pharmacol. Sin. 38 (2017) 798–805.

[30] B. Zhu, J. Travas-Sejdic, PNA versus DNA in electrochemical gene sensing based on conducting polymers: study of charge and surface blocking effects on the sensor signal, Analyst 143 (2018) 687–694.

[31] M. Xu, S. Xing, X. Xu, P. Fu, W. Xu, C. Zhao, Label-free colorimetric aptasensor for highly sensitive and selective detection of proteins by using PNA/DNA hybrids and a cyanine dye, Anal. Methods 10 (2018) 3824–3829.

[32] W. Xu, S. Xing, X. Xu, M. Xu, P. Fu, T. Gao, C. Zhao, peptide nucleic acid-assisted label-free detection of single-nucleotide polymorphisms based on light scattering of carbon nanotubes, ACS Omega 3 (2018) 17835–17841.

[33] X.D. Su, R. Kanjanawarut, Control of metal nanoparticles aggregation and dispersion by PNA and PNA−DNA complexes and its application for colorimetric DNA detection, ACS Nano 3 (2009) 2751–2759.

[34] R. Kanjanawarut, X.D. Su, Colorimetric detection of DNA using unmodified metallic nanoparticles and peptide nucleic acid probes, Anal. Chem. 81 (2009) 6122–6129.

[35] V.G. Joshi, K. Chindera, A.K. Singh, A.P. Sahoo, V.D. Dighe, D. Thakuria, A.K. Tiwari, S. Kumar, Rapid label-free visual assay for the detection and quantification of viral RNA using peptide nucleic acid (PNA) and gold nanoparticles (AuNPs), Anal. Chim. Acta 795 (2013) 1–7.

[36] X. Li, J. Song, B.L. Chen, B. Wang, R. Li, H.M. Jiang, J.F. Liu, C.Z. Li, A label-free colorimetric assay for detection of c-Myc mRNA based on peptide nucleic acid and silver nanoparticles, Sci. Bull. 61 (2016) 276–281.

[37] P. Teengam, W. Siangproh, A. Tuantranont, T. Vilaivan, O. Chailapakul, C.S. Henry, Multiplex paper-based colorimetric DNA sensor using pyrrolidinyl peptide nucleic acid-induced AgNPs aggregation for detecting MERS-CoV, MTB, and HPV oligonucleotides, Anal. Chem. 89 (2017) 5428–5435.

[38] W. Haiss, N.T.K. Thanh, J. Aveyard, D.G. Fernig, Determination of size and concentration of gold nanoparticles from UV-vis spectra, Anal. Chem. 79 (2007) 4215–4221.

[39] J. Yguerabide, E.E. Yguerabide, Light-scattering submicroscopic particles as highly fluorescent analogs and their use as tracer labels in clinical and biological applications. I. Theory, Anal. Biochem. 262 (1998) 137–156.

[40] J. Yguerabide, E.E. Yguerabide, Light-scattering submicroscopic particles as highly fluorescent analogs and their use as tracer labels in clinical and biological applications. II. Experimental characterization, Anal. Biochem. 262 (1998) 157–176.

[41] K.C. Grabar, R.G. Freeman, M.B. Hommer, M.J. Natan, Preparation and characterization of Au colloid monolayers, Anal. Chem. 67 (1995) 735–743.

[42] R.C. Doty, T.R. Tshikhudo, M. Brust, D.G. Fernig, Extremely stable water-soluble Ag nanoparticles, Chem. Mater. 17 (2005) 4630–4635.

[43] B.S. Gaylord, M.R. Massie, S.C. Feinstein, G.C. Bazan, SNP detection using peptide nucleic acid probes and conjugated polymers: applications in neurodegenerative disease identification, Proc. Natl. Acad. Sci. U. S. A. 102 (2005) 34–39.

[44] M. Komiyama, S. Ye, X. Liang, Y. Yamamoto, T. Tomita, J.-M. Zhou, H. Aburatani, PNA for one-base differentiating protection of DNA from nuclease and its use for SNPs detection, J. Am. Chem. Soc. 125 (2003) 3758–3762.

[45] B. Ren, J.-M. Zhou, M. Komiyama, Straightforward detection of SNPs in double-stranded DNA by using exonuclease III/nuclease s1/PNA system, Nucleic Acids Res. 32 (2004) e42.

[46] V. Demidov, M.D. Frank-Kamenetskii, M. Egholm, O. Buchardt, P.E. Nielsen, Sequence selective double strand DNA cleavage by Peptide Nucleic Acid (PNA) targeting using nuclease S1, Nucleic Acids Res. 21 (1993) 2103–2107.

[47] J. Sambrook, D. Russell, Molecular Cloning: A Laboratory Manual, 3rd ed., Cold Spring Harbor Lab. Press, Plainview, NY, 2001, pp. A4.1–A4.52.

[48] F. Aboul-ela, D. Koh, I.J. Tinoco, F.H. Martin, Base-base mismatches. Thermodynamics of double helix formation for dCA3XA3G + dCT3YT3G (X, Y = A,C,G,T), Nucleic Acids Res. 13 (1985) 4811–4824.

[49] S. Ikuta, K. Takagi, B.R. Wallace, K. Itakura, Dissociation kinetics of 19 base paired oligonucleotide-DNA duplexes containing different single mismatched base pairs, Nucleic Acids Res. 15 (1987) 797–811.

[50] Y. Li, A.W. Wark, H.J. Lee, R.M. Corn, Single-nucleotide polymorphism genotyping by nanoparticle-enhanced surface plasmon resonance imaging measurements of surface ligation reactions, Anal. Chem. 78 (2006) 3158–3164.